Advances in Nano Research, *Vol. 9, No. 4 (2020) 251-261*
DOI: https://doi.org/10.12989/anr.2020.9.4.251

Vibration of SWCNTs: Consistency and behavior of polynomial law index with Galerkin's model

Mohamed A. Khadimallah[1,2], Muzamal Hussain*[3], Khaled Mohamed Khedher[4,5], Souhail Mohamed Bouzgarrou[6], Abdullah F. Al Naim[7], Muhammad Nawaz Naeem[3], Muhammad Taj[8], Zafar Iqbal[9,10] and Abdelouahed Tounsi[11,12]

[1]*Prince Sattam Bin Abdulaziz University, College of Engineering, Civil Engineering Department, BP 655, Al-Kharj, 11942, Saudi Arabia*
[2]*Laboratory of Systems and Applied Mechanics, Polytechnic School of Tunisia, University of Carthage, Tunis, Tunisia*
[3]*Department of Mathematics, Government College Universit Faisalabad, Punjab, Pakistan*
[4]*Department of Civil Engineering, College of Engineering, King Khalid University, Abha 61421, Saudi Arabia*
[5]*Department of Civil Engineering, High Institute of Technological Studies, Mrezgua University Campus, Nabeul 8000, Tunisia*
[6]*Civil Engineering Department, Faculty of Engineering, Jazan University, Kingdom of Saudi Arabia*
[7]*Department of Physics, College of Science, King Faisal University, P.O. Box 400, Al-Ahsa 31982, Saudi Arabia*
[8]*Department of Mathematics, University of Azad Jammu and Kashmir, Muzaffarabad, 1300, Azad Kashmir, Pakistan*
[9]*Department of Mathematics, University of Sargodha, Sargodha, Punjab, Pakistan*
[10]*Department of Mathematics, University of Mianwali, Punjab, Pakistan*
[11]*YFL (Yonsei Frontier Lab), Yonsei University, Seoul, Korea*
[12]*Department of Civil and Environmental Engineering, King Fahd University of Petroleum & Minerals, 31261 Dhahran, Eastern Province, Saudi Arabia*

(*Received April 4, 2020, Revised September 23, 2020, Accepted September 28, 2020*)

Abstract. In this article, vibration attributes of single walled carbon nanotubes based on Galerkin's method have been investigated. The influence of power law index subjected to different end supports has been overtly examined. Application of the Hamilton's variational principal leads to the formation of partial differential equations. The effects of different physical and material parameters on the fundamental frequencies are investigated for armchair and zigzag carbon nanotubes with clamped-clamped, simply supported and clamped-free boundary conditions. By using volume fraction for power law index, the fundamental natural frequency spectra for two forms of Single-Walled Carbon Nanotubes (SWCNTs) are calculated. The influence of frequencies against length-to-diameter ratios with varying power law index are investigated in detail for these tubes. MATLAB software package has been utilized for extracting tube frequency spectra. The obtained results are confirmed by comparing with available literature.

Keywords: frequency spectra; volume fraction; polynomial law; clamped support

1. Introduction

Basically, Carbon Nanotubes (CNTs) are in shape of cylindrical macromolecules composed of carbon atoms attracted astounding response from scientific community. Over the last number of years, CNTs have become focus of interest amidst leading scientists from many research areas. Since from the last decade CNTs have become potential subject of scientific research with its vigorous performance in the various fields.

Owing to remarkable physical and mechanical features of the nanosized structures, they have been persuasive and contemporary measure in aerospace, microscopic system, actuators, gas exposure, defence, diagnosis devices and several others. Here, a succinct review has been provided regarding different applications of CNTs. Their enormous versatility has made them being coined as a solution looking for problems. CNTs have potential use in the industry and engineering fields such as mechanical, civil, aerospace as load bearing instrument for ships, building and aircrafts, etc. CNTs have a variety of uses and applications in potential looking fields, some of which are charge detectors, electronics, communication, composite materials, biotechnology, environment, energy storage, chemical and optical. Natuski *et al*. (2006) conducted the vibration of nested CNTs in elastic matrix. Flügge shell theory again had been engaged to establish administrative shell equations while proposed method was wave propagation. Bensattalah *et al*. (2018) studied the critical buckling of a Single-Walled Carbon Nanotube (SWCNT) embedded in Kerr's medium is studied. Based on the nonlocal continuum theory and the Euler-Bernoulli beam model. The governing equilibrium equations are acquired and solved for CNTs subjected to mechanical loads and embedded in Kerr's medium. Kerr-type model is employed to simulate the interaction of the SWNT with a surrounding elastic medium. Wang and Liew (2007) studied nano- and micro-tubes using EBM and TBM. The results showed that to indicate the importance of

*Corresponding author, Ph.D.,
E-mail: muzamal45@gmail.com;
muzamalhussain@gcuf.edu.pk

ISSN: 2287-237X (Print), 2287-2388 (Online)

applied theory of beams, the shear effect is evident for the CNTs. Furthermore, vibrations of nanotubes have been modeled by atomistic/continuum models. The fundamental frequencies of CNTs have higher values at lower diameter and showed that the chirality have no momentous influence on frequencies of nanotubes. The vacancies are produced due to holes in the graphite structure and due to chemical and theoretical physics, the defects in CNTs reduce the Young's modulus (Kotakoski *et al*. 2006, Usuki and Yogo 2009) formed beam equations again based on Flügge shell theory, they concluded that if nonlocality and refined model are ignored then the generalized beam theory and Flügge theory produce alike results. Owing to this, Gibson *et al*. (2007) presented a coherent review about the simulations, and modeling of vibrating nanotubes. Akbaş (2017a, b) investigated the free vibration analysis of edge cracked cantilever microscale beams composed of Functionally Graded Material (FGM) based on the Modified Couple Stress Theory (MCST). The material properties of the beam are assumed to change in the height direction according to the exponential distribution. The FG nanobeam is excited by a transverse triangular force impulse modulated by a harmonic motion. Kulathunga *et al*. (2009) widely explored the classical shell theory to compute the strain of SWCNTs. It has been calculated for the first time from this formula in the absence of length-diameter ratio, the critical buckling strain can be calculated. The results are verified with the Molecular Dynamics (MD) simulation based on compass force field. This improved formula shows a significant error at the smaller diameters and higher aspect ratios. Hamidi *et al*. (2018) investigated the non-local Timoshenko beam theory for the free vibration of armchair single-walled carbon nanotubes embedded in elastic medium including the thermal effects. The mechanical properties of nano-composite (carbon nanotubes and polymer matrix) are treated as functions of temperature change and the analytical solution is derived according to the governing equations of non-local Timoshenko beam models. Akbaş (2016a, b) studied the forced vibration analysis of a simple supported viscoelastic nanobeam based on MCST. The nanobeam is excited by a transverse triangular force impulse modulated by a harmonic motion. The elastic medium is considered as Winkler-Pasternak elastic foundation. The static bending of edge cracked micro beams is studied analytically under uniformly distributed transverse loading based on MCST. Selim (2010) performed vibrational behavior of SWCNT with compression stresses using multilayers. The motion equation was derived for the vibration analysis of SWCNTs using wave propagation. However, the outcomes of this research noted for various structures and the overall electronic and structural properties.

Rouhi *et al*. (2013) executed the axial buckling of double-walled CNT subject to various layer-wise conditions by using Rayleigh-Ritz based upon nonlocal Flügge shell theory. Their study showed that the number of different layer-wise boundary conditions dominates the choice of values for nonlocal parameter. Moghadam *et al*. (2014) scrutinized the frequencies of SWCNTs using molecular mechanics approach with various parameters. The frequency outcomes revealed the frequencies increases or decreases with the orientation of carbon-carbon bond.

Fenjan *et al*. (2020) utilized the Differential Quadrature (DQ) method for investigating free vibrations of porous Functionally Graded (FG) micro/nano beams in thermal environments. The exact location of neutral axis in FG material has been assumed where the material properties are described via porosity-dependent power-law functions. A scale factor related to couple stresses has been employed for describing size effect. Akbaş (2018a, b, c) investigated the forced vibration analysis of a cracked functionally graded microbeam using modified couple stress theory with damping effect. Mechanical properties of the functionally graded beam change vary along the thickness direction. The Kelvin-Voigt model is considered in the damping effect. In solution of the dynamic problem, finite element method is used within Timoshenko beam theory in the time domain. Madani *et al*. (2016) studied the vibration of FG-CNT-reinforced piezoelectric cylindrical shells utilizing the method of differential quadrature. The mixture rule of four distribution types was used in the thickness direction. Avcar (2019) conducted the influence of various volume fraction laws using the classical theory for FG beam. By varying the volume fraction laws, the span-to-depth ratio versus frequencies was examined in detail. The frequencies for span to depth ratio with varying volume fraction index were examined in detail. Abdulrazzaq *et al*. (2020) thermo-elastic buckling of small scale FGM nano-size plates with clamped edge conditions rested on an elastic substrate exposed to uniformly, linearly and non-linearly temperature distributions have been investigated employing a secant function based refined theory. Material properties of the FGM nano-size plate have exponential gradation across the plate thickness. Semmah *et al*. (2019) studied the buckling analysis of zigzag single walled boron nitride based on Winkler foundation. Effect of different nonlocal parameter was investigated with closed form solution.

The suggested method to investigate the solution of fundamental eigen relations is Galerkin's method, which is a well-known and efficient technique to develop the fundamental frequency equations. It is keenly seen from the literature, no evidence is found concerning current model. The specific influence of three different end supports based on Galerkin's such as Clamped-Clamped (C-C), Simply Supported-Simply Supported (SS-SS) and Clamped-Free (C-F) is tested in detail.

Researchers have used many numerical techniques for the vibration of CNTs, nanobeams and nanoplates as a smart structures (Tohidi *et al*. 2018, Arefi and Zenkour 2017, Arani *et al*. 2016, Krommer *et al*. 2016, Yeh 2016) and for other structures (AlSaleh and Fuggini 2020, Lee *et al*. 2019, Zahrai and Kakouei 2019, Poplawski *et al*. 2019, Eltaher *et al*. 2019, Ebrahimi *et al*. 2019, Safaei *et al*. 2019, Shahsavari *et al*. 2019, Benmansour *et al*. 2019, Batou *et al*. 2019, Salah *et al*. 2019, Nebab *et al*. 2019, Akbaş 2015, 2016c, 2019a, b, 2020). Moreover, computer computations have been used by many researchers in literature through different models to examine vibrational characteristics of CNTs (and or SWCNTs) and nanostructures. The method of

choice on nano-level to study the fundamental natural frequencies of SWCNTs with different parameters using Galerkin's method is best choice and popular tool for different theories. In addition, in order to estimate the natural frequency of SWCNTs, new models based on Galerkin's method have been shown to converge faster than beam models and other numerical techniques. Therefore, these Galerkin's method-based models are another better option to utilize the research technique of CNTs with the result that within the limits of acceptable statistical error and mathematical rigors than the earlier used methods/ simulations. This study extends the different models based on Galerkin's method to calculate the fundamental frequency of SWCNTs which is our particular motive.

The particular motivation of our work is to investigate vibrations characteristics of armchair and zigzag SWCNT by means of Galerkin's method with polynomial volume fraction law. Vibrations of SWCNTs for armchair (11, 11) and zigzag (13, 0) have been analyzed with specified conditions. We have developed a new model from the combination of the extended Love shell theory with Galerkin's method. It has been shown that frequency curves increase as an increment in the power law index The specific influence of three different end supports Clamped-Clamped (C-C), Simply Supported-Simply Supported (SS-SS) and Clamped-Free supported (C-F) is examined in detail. This method has been developed to converge more quickly than other methods and models. It is investigated the effect of frequencies against length-to-diameter ratio/ aspect ratio by varying polynomial law index.

2. Theoretical investigations

The indices of armchair and zigzag occur during the rolling of tube. Fig. 1 shows the schema of the indices as (m, n) which occurs on rolling of the tube and these indices formed as armchair and zigzag, if $m = n$, $n = 0$, respectively.

The motion of FG-CNT is subjected to the produce the resultant forces and the moments and these forces are expressed as

$$\begin{aligned}(N_{xx}, N_{\theta\theta}, N_{x\theta}) &= \int_{\frac{-h}{2}}^{\frac{h}{2}} (\sigma_{xx}, \sigma_{\theta\theta}, \sigma_{x\theta}) dz \\ (M_{xx}, M_{\theta\theta}, M_{x\theta}) &= \int_{\frac{-h}{2}}^{\frac{h}{2}} (\sigma_{xx}, \sigma_{\theta\theta}, \sigma_{x\theta}) z dz\end{aligned} \tag{1}$$

where σ_{xx} and $\sigma_{\theta\theta}$ exhibits the stress components in the axial and tangential directions respectively and $\sigma_{x\theta}$ designates the shear stress in the $x\theta$-plane.

For CNTs, according to two dimensional Hook's law, the entries of stress vector can be defined in Eq. (1) as

$$\begin{pmatrix}\sigma_{xx}\\ \sigma_{\theta\theta}\\ \sigma_{x\theta}\end{pmatrix} = \begin{bmatrix}S_{11} & S_{12} & 0\\ S_{12} & S_{22} & 0\\ 0 & 0 & S_{66}\end{bmatrix}\begin{pmatrix}e_{xx}\\ e_{\theta\theta}\\ e_{x\theta}\end{pmatrix} \tag{2}$$

Similarly, e_{xx} and $e_{\theta\theta}$ represent the strain in x- and θ-directions whereas $e_{x\theta}$ indicates the shear strain in the $x\theta$-plane (Fig. 2).

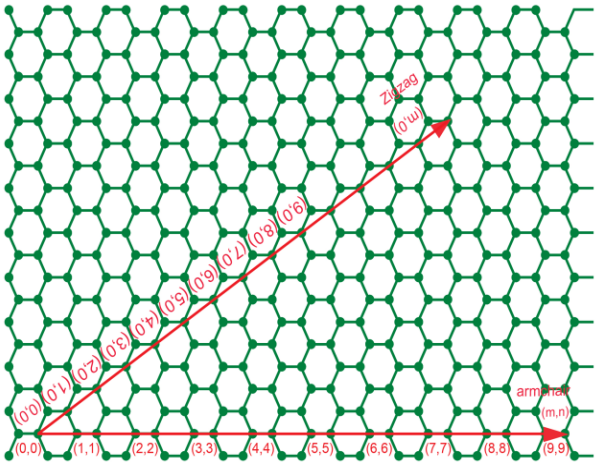

Fig. 1 Hexagonally description of armchair and zigzag SWCNTs on the graphene sheet

The strain energy for CNT is

$$H = \int_0^L \int_0^{2\pi} [\delta]^T [S][\mu] \frac{R}{2} d\theta\, dx \tag{3}$$

where

$$\{\delta\}^T = \{\varsigma_1 \quad \varsigma_2 \quad \tau \quad \zeta_1 \quad \zeta_2 \quad 2\xi\} \tag{4}$$

whereas $(\varsigma_1, \varsigma_2, \tau)$ and $(\zeta_1, \zeta_2, 2\xi)$ are referenced as surface curvature and surface strains.

And $[S]$ represents the matrices of reduced stiffness and is expressed by

$$[S] = \begin{pmatrix}F & G\\ G & K\end{pmatrix} \tag{5}$$

where the sub-matrices F, G and K with their entries are listed as

$$F = \begin{pmatrix}F_{11} & F_{12} & 0\\ F_{12} & F_{22} & 0\\ 0 & 0 & F_{66}\end{pmatrix} \tag{6a}$$

$$G = \begin{pmatrix}G_{11} & G_{12} & 0\\ G_{12} & G_{22} & 0\\ 0 & 0 & G_{66}\end{pmatrix} \tag{6b}$$

$$K = \begin{pmatrix}K_{11} & K_{12} & 0\\ K_{12} & K_{22} & 0\\ 0 & 0 & \mathrm{K}_{66}\end{pmatrix} \tag{6c}$$

The complete form of the matrix $[S]$ is obtained as

$$[\mathrm{S}] = \begin{pmatrix}F_{11} & F_{12} & 0 & G_{11} & G_{12} & 0\\ F_{12} & F_{22} & 0 & G_{12} & G_{22} & 0\\ 0 & 0 & F_{66} & 0 & 0 & G_{66}\\ G_{11} & G_{12} & 0 & K_{11} & K_{12} & 0\\ G_{12} & G_{22} & 0 & K_{12} & K_{22} & 0\\ 0 & 0 & K_{66} & 0 & 0 & K_{66}\end{pmatrix} \tag{7}$$

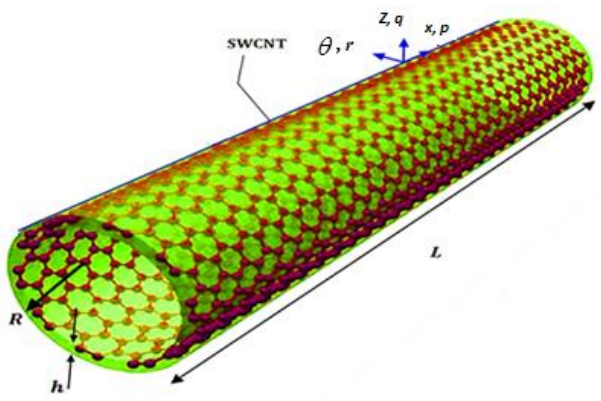

Fig. 2 Geometry of CNT

where the membrane (F_{lm}), coupling (G_{lm}) and flexural (K_{lm}) stiffness are expressed as

$$F_{lm} = \int_{\frac{-h}{2}}^{\frac{h}{2}} S_{lm} dz$$
$$G_{lm} = \int_{\frac{-h}{2}}^{\frac{h}{2}} z S_{lm} dz \, , K_{lm} = \int_{\frac{-h}{2}}^{\frac{h}{2}} z^2 S_{lm} dz \tag{8}$$

For isotropic CNTs the coupling stiffness G_{lm} condensed to zero when its material is isotropic and does not become zero when a tube is structured from composite or laminated or functionally graded material.

S_{lm} is reduced stiffness for isotropic materials with conjunction of E and v are written as

$$S_{11} = S_{22} = \frac{E}{1-\nu^2}, \qquad S_{12} = \frac{\nu E}{1-\nu^2}, \qquad S_{66} = \frac{E}{2(1+\nu)} \tag{9}$$

$$\begin{aligned} H = \frac{1}{2}\int_0^L \int_0^{2\pi} \{ & F_{11}{\varsigma_1}^2 + F_{22}{\varsigma_2}^2 + 2F_{12}\varsigma_1\varsigma_2 + F_{66}\tau^2 \\ & + 2G_{11}\varsigma_1\zeta_1 + 2G_{12}\varsigma_1\zeta_2 + 2G_{12}\varsigma_2\zeta_1 + 2G_{22}\varsigma_2\zeta_2 \\ & + 4G_{66}\tau\xi + K_{11}{\zeta_1}^2 + K_{22}{\zeta_2}^2 + 2K_{12}\zeta_1\zeta_2 \\ & + 4K_{66}\xi^2 \} Rd\theta dx \end{aligned} \tag{10}$$

With advancements in study of CNT problem, new shell theories were developed and used to do vibration analysis of CNT problems. There found minute differences in numerical results when different shell theories were utilized. Applying Love shell theory, strain-displacement expressions are stated as

$$\{\varsigma_1, \varsigma_2, \tau\} = \left\{\frac{\partial p}{\partial x}, \qquad \frac{1}{R}\left(\frac{\partial q}{\partial \theta} + w\right), \qquad \frac{\partial q}{\partial x} + \frac{1}{R}\frac{\partial p}{\partial \theta}\right\} \tag{11}$$

Similarly, relations for curvature-displacement for ζ_1, ζ_2, ξ are written as

$$\left\{ \{\zeta_1, \zeta_2, \xi\} = \begin{Bmatrix} -\frac{\partial^2 r}{\partial x^2}, & -\frac{1}{R^2}\left(\frac{\partial^2 r}{\partial \theta^2} - \frac{\partial q}{\partial \theta}\right), \\ -\frac{1}{R}\left(\frac{\partial^2 r}{\partial x \partial \theta} - \frac{\partial q}{\partial x}\right) \end{Bmatrix} \right\} \tag{12}$$

On substitution of the Eqs. (11) and (12) in the relation of Eq. (9), the strain energy H in modified form can be elaborated as

$$\begin{aligned} H = \frac{1}{2}\iint_0^{2\pi L} [& F_{11}\left(\frac{\partial p}{\partial x}\right)^2 + F_{22}\frac{1}{R^2}\left(\frac{\partial q}{\partial \theta} + r\right)^2 + 2F_{12}\frac{1}{R}\frac{\partial p}{\partial x} \\ & \left(\frac{\partial q}{\partial \theta} + r\right) + F_{66}\left(\frac{\partial v}{\partial \theta} + \frac{1}{R}\frac{\partial p}{\partial x}\right)^2 - 2G_{11}\left(\frac{\partial p}{\partial x}\right)\left(\frac{\partial^2 r}{\partial x^2}\right) \\ & -2G_{12}\frac{1}{R^2}\left(\frac{\partial p}{\partial x}\right)\left(\frac{\partial^2 r}{\partial \theta^2} - \frac{\partial q}{\partial \theta}\right) - 2G_{12}\frac{1}{R}\left(\frac{\partial q}{\partial \theta} + r\right) \\ & \left(\frac{\partial^2 r}{\partial x^2}\right) - 2G_{22}\frac{1}{R^3}\left(\frac{\partial q}{\partial \theta} + r\right)\left(\frac{\partial^2 r}{\partial \theta^2} - \frac{\partial q}{\partial \theta}\right) - 4G_{66}\frac{1}{R} \\ & \left(\frac{\partial q}{\partial \theta} + \frac{1}{R}\frac{\partial p}{\partial x}\right)\left(\frac{\partial^2 r}{\partial x \partial \theta} - \frac{3}{4}\frac{\partial q}{\partial x} + \frac{1}{4R}\frac{\partial p}{\partial \theta}\right) + K_{11}\left(\frac{\partial^2 r}{\partial x^2}\right)^2 \\ & \frac{D_{22}}{R^4}\left(\frac{\partial^2 r}{\partial \theta^2} - \frac{\partial q}{\partial \theta}\right)^2 + 2K_{12}\frac{1}{R^2}\left(\frac{\partial^2 r}{\partial x^2}\right)\left(\frac{\partial^2 r}{\partial \theta^2} - \frac{\partial q}{\partial \theta}\right) \\ & 4K_{66}\frac{1}{R^2}\left(\frac{\partial^2 r}{\partial x \partial \theta} - \frac{3}{4}\frac{\partial q}{\partial x} + \frac{1}{4R}\frac{\partial p}{\partial \theta}\right)^2] Rdxd\theta \end{aligned} \tag{13}$$

Similarly, kinetic energy for CNTs doing vibration is written as

$$M = \frac{1}{2}\iint_0^{2\pi L} \rho_T \left[(\frac{\partial p}{\partial t})^2 + (\frac{\partial q}{\partial t})^2 + (\frac{\partial r}{\partial t})^2 \right] Rdxd\theta \tag{14}$$

The mass density relation ε_t is expressed as

$$\varepsilon_t = \int_{-h/2}^{h/2} \rho dz \tag{15}$$

With the coalescence energies (strain and kinetic), the Lagrangian functional can be obtained can be given as

$$\Omega = M - H \tag{16}$$

where Ω designates the Lagrangian functional. Substituting Eqs. (13) and (14) into the Eq. (16) and making the use of Hamiltonian variational principle Sodel (1981) to the Lagrange energy functional. Application of the variation principal leads to the formation of partial differential equations.

Many material researchers have used various methods to solve PDEs. Closed form functions exist for solutions of tube motion equations for some types of edge conditions. For rest of boundary conditions, the numerical solutions are obtained by approximate methods. Galerkin's method is made to extract approximate solution of tube controlling equations because these techniques provide results robustly with sufficient accuracy. This method is appropriate, straightforward to extract the tube vibration frequencies. Differential equations are generated involving the three dependent variables. Boundary conditions existing at the tube ends are met by these functions. For solving the tube problem, first the special variables x, θ and temporal variable t are split. For this purpose, the following modal displacement expressions for the deformation functions are

Table 1 Convergence of C-C frequencies with frequency parameter $\lambda = \omega R\sqrt{(1-\nu^2)\varepsilon/E}$ (Xuebin 2008)

Method	n			
	2	3	4	5
Xuebin (2008)	0.014052	0.022726	0.042272	0.068116
Present	0.014256	0.022713	0.042215	0.06805

Table 2 Comparison for isotropic tube with Moazzez *et al*. (2018)

m	Method	N				
		1	2	3	4	5
1	Moazzez *et al.* (2018)	3.81	10.87	22.02	39.00	61.21
	Present	3.86	10.91	22.19	39.29	61.43

p, q and r. According to the first order shear deformation theory, the displacement components are represented in the form (Flügge 1962, Forsberg 1962)

$$p(x,\theta,t) = \frac{d\chi}{dx} d_m \sin n\theta \cos \omega t \tag{17a}$$

$$q(x,\theta,t) = \chi(x) e_m \cos n\theta \cos \omega t \tag{17b}$$

$$r(x,\theta,t) = \chi(x) f_m \sin n\theta \cos \omega t \tag{17c}$$

where the parameters d_m, e_m and f_m in Eqs. (17a)-(17c) represents the vibration in the x , θ and z directions correspondingly. $\chi(x)$ signifies the unknown axial deformation function that fulfills the end conditions stated at two tube ends. Making substitutions of the expressions for the deformation displacement functions with their corresponding derivatives, and multiplying with $\frac{d\chi}{dx}$, and $\chi(x)$ respectively. We attained an equation after integrating x from 0 to L.

Making the arrangement of terms in Eqs. (17a)-(17c), the tube frequency equation framed in the eigenvalue form as below.

$$\left.\begin{aligned} \sigma_{11} d_m + \sigma_{12} e_m + \sigma_{13} f_m &= -\omega^2 \varepsilon h d_m I_2 \\ \sigma_{21_{dm}} + \sigma_{22} e_m + \sigma_{23} f_m &= -\omega^2 \varepsilon h e_m I_4 \\ \sigma_{31} d_m + \sigma_{32} e_m + \sigma_{33} f_m &= -\omega^2 \varepsilon h f_m I_{13} \end{aligned}\right\} \tag{18}$$

Here terms $\sigma_{ij}(i,j=1,2,3)$ implicate geometrical and material quantities and are tabulated in the Appendix-I. The above equations can be arranged in matrices form as

$$\begin{pmatrix} \sigma_{11} & \sigma_{12} & \sigma_{13} \\ \sigma_{21} & \sigma_{22} & \sigma_{23} \\ \sigma_{31} & \sigma_{32} & \sigma_{33} \end{pmatrix} \begin{pmatrix} d_m \\ e_m \\ f_m \end{pmatrix} + \omega^2 \varepsilon h \begin{pmatrix} I_2 & 0 & 0 \\ 0 & I_4 & 0 \\ 0 & 0 & I_{13} \end{pmatrix} \begin{pmatrix} d_m \\ e_m \\ f_m \end{pmatrix} = 0 \tag{19}$$

2.1 Polynomial volume fraction law

The volume fraction V_{cnt} are designated for CNTs, respectively. According to Shen (2009), the material property for composite material occurs which is called the polynomial volume fraction law. In this law, ∇ and h is designated for power law index and thickness, where z is the coordinate which varies from zero to infinity. The material distribution according to Shen (2009).

$$V_{cnt} = \left[\frac{2Z+h}{2h}\right]^{\nabla} V_{tcnt} \tag{20}$$

3. Results and discussion

For the convergence rate of CNT, the non-dimensional frequency parameters enumerated in the current work, i.e., using Galerkin's method, are happened to be in a good consistency along with the so-called exact results furnished by (Xuebin 2008, Moazzez *et al.* 2018), those were established by working out with three boundary conditions as provided in Tables 1-2. The proposed model based on Galerkin's method can incorporate in order to accurately predict the acquired results of material data point and the percentage difference is negligible.

Here, the frequencies for CNT are evaluated with exponential volume fraction law under C-C, C-F and SS-SS supported with height-to-diameter ratio $h{:}d$ = 0.002 m. Table 3 displays CNT frequencies with the end conditions of C-C under polynomial volume fraction. In this Table, n is increased almost two times as compared to the edge condition of SS-SS at the initial value of n but almost its values become similar at n = 5.

Table 4 depict the frequencies versus the axial wave number CNT for C-C conditions. The polynomial volume fraction law has great influence on the frequency. When the value of ∇ is increased then as a result the corresponding natural frequency (THz) becomes smaller gradually. Table 5 shows the variations of C-C frequencies versus the $L{:}d$ and $h{:}d$ for CNTs. In these Tables, a great influence of ∇ has been seen on the variation of natural frequency. Tables 6-8

Table 3 C-C frequencies against the circumferential wave number (n) ($h{:}d$ = 0.002 m, $L{:}d$ = 20 m)

n	∇ = 0.5			∇ = 1			∇ = 8		
	S-S	C-C	C-F	S-S	C-C	C-F	S-S	C-C	C-F
1	13.213	28.292	5.41	13.142	28.141	5.382	12.95	27.73	5.303
2	4.472	9.913	2.08	4.446	9.858	2.069	4.384	9.716	2.039
3	4.15	5.95	3.698	4.125	5.916	3.678	4.07	5.834	3.627
4	7.041	7.464	6.951	7.001	7.421	6.913	6.905	7.32	6.817
5	11.253	11.369	11.223	11.191	11.306	11.162	11.036	11.15	11.006

Table 4 C-C frequencies against axial wave mode (m) (n = 1, $h:d$ = 0.002 m, $L:d$ = 20 m)

m	∇ = 0.5			∇ = 1			∇ = 8		
	S-S	C-C	C-F	S-S	C-C	C-F	S-S	C-C	C-F
1	13.213	28.292	5.052	13.142	28.141	5.025	12.95	27.73	4.951
2	48.48	69.643	29.663	48.221	69.271	29.505	47.517	68.259	29.074
3	97.295	120.07	74.424	96.776	119.43	74.027	95.362	117.68	72.945
4	152.73	174.62	128.88	151.92	173.7	128.2	149.7	171.15	126.32
5	210.48	230.33	187.53	209.36	229.11	186.52	206.3	225.75	183.8

Table 5 C-C frequencies against $L:d$

$L:d$	∇ = 0.5			∇ = 1			∇ = 8		
	S-S	C-C	C-F	S-S	C-C	C-F	S-S	C-C	C-F
1	669.14	722.53	558.9	689.44	28.141	555.92	679.37	27.73	549.02
2	469.27	518.23	276.16	466.77	69.271	274.69	459.95	68.259	270.68
3	152.73	215.33	69.25	151.92	119.43	68.881	149.7	117.68	67.874
4	89.786	143.05	38.037	89.306	173.69	37.833	88.001	171.15	37.281
5	48.48	87.567	19.497	48.221	229.1	19.393	47.517	225.75	19.11

Table 6 Frequency comparison of C-C armchair and zigzag CNTs versus $L:d$ with index of polynomial law

$L : d$	(6, 6)			(8, 0)		
	∇ = 0.5	∇ = 1	∇ = 1.5	∇ = 0.5	∇ = 1	∇ = 1.5
4.86	145.62	145.99	146.20	91.51	91.81	91.512
6.67	137.57	137.92	138.12	66.416	66.584	66.679
8.47	133.96	134.31	134.49	52.302	52.434	52.509
10.26	132.05	132.238	132.57	43.177	43.286	43.348
13.89	130.16	130.49	130.67	31.893	31.973	32.019
17.49	129.31	129.64	129.82	25.328	25.392	25.428
21.06	128.86	129.11	129.37	21.0135	21.088	21.118
24.66	128.59	128.91	129.10	17.964	18.009	18.035
28.31	128.41	128.76	128.92	15.648	15.687	15.710
31.85	128.29	128.62	128.80	13.908	13.944	13.963
35.53	128.21	128.47	128.72	12.468	12.499	12.517

show the frequency comparison of armchair and zigzag CNTs with varying different exponent of polynomial law. In these tables, frequencies' values are tabulated for three different boundary conditions. It is observed that on enhancing the values of $L:d$, frequencies decreas for three boundary conditions. On increasing the exponent of polynomial law, the frequency values increase. The armchair values for C-C (see Table 6), SS-SS (see Table 7) and C-F (see Table 8) are greater than that of zigzag values with same conditions. The fundamental natural frequencies of armchair (11, 11) and zigzag (13, 0) SWCNTs with specified boundary conditions is obtained using Galerkin's method. Fig. 3 shows the frequency response of armchair versus $L: d$ for different values of power law index ∇ = 0.5, 1, 1.5. The results for armchair and zigzag SWCNTs are investigated for different computation with Boundary Conditions (BCs). The fundamental natural frequencies of armchair (11, 11), and zigzag (13, 0) for C-C, SS-SS and C-F conditions are investigated. It is found that from these figures that the frequency outcomes of C-C frequencies are higher than SS-SS, C-F for varying $L:d$ and the frequencies increase on increasing the power law index.

Variation of frequencies versus length for indices (13, 0), with BCs has been plotted in graph of Fig. 3. The value of fundamental frequency decreases on increasing the ratio of length-to-diameter of the tube. In addition, when the tube length-to-diameter ratio increases from 5~10, the frequency decreases rapidly, while for the length-to-diameter ratio ($L:d$ = 10~15), the frequency is gently parallel. In present result, the frequencies are significant at length-to-diameter ratio ($L\ d$ = 35). It shows that natural frequencies decrease as $L:d$ is increased, for these boundary conditions. For long

Table 7 Frequency comparison of SS-SS armchair and zigzag CNTs versus *L:d* with index of polynomial law

L : d	(6, 6)			(8, 0)		
	∇ = 0.5	∇ = 1	∇ = 1.5	∇ = 0.5	∇ = 1	∇ = 1.5
4.86	143.13	143.49	143.70	85.790	86.006	86.128
6.67	136.18	136.52	136.72	62.509	62.667	62.757
8.47	133.08	133.41	133.60	49.225	49.349	49.420
10.26	131.44	131.77	131.96	40.637	40.739	40.798
13.89	129.82	130.15	130.33	30.017	30.093	30.136
17.49	129.10	129.42	129.61	23.838	23.898	23.933
21.06	128.71	129.04	129.22	19.797	19.847	19.876
24.66	128.48	128.89	128.99	16.907	16.950	16.974
28.31	128.33	128.65	128.84	14.727	14.764	14.785
31.85	128.23	128.55	128.74	13.090	13.123	131.42
35.53	128.16	128.48	128.66	11.734	11.764	11.781

Table 8 Frequency comparison of C-F armchair and zigzag CNTs versus *L:d* with index of polynomial law

L : d	(6, 6)			(8, 0)		
	∇ = 0.5	∇ = 1	∇ = 1.5	∇ = 0.5	∇ = 1	∇ = 1.5
4.86	140.80	141.16	141.36	80.428	80.631	80.746
6.67	134.88	135.22	135.42	58.602	58.750	58.834
8.47	132.26	132.59	132.78	46.148	46.265	46.331
10.26	130.87	131.20	131.39	38.097	38.193	38.248
13.89	129.51	129.83	130.02	28.141	28.212	38.252
17.49	128.90	129.22	129.41	22.348	22.405	22.437
21.06	128.58	128.90	129.08	18.560	18.607	18.633
24.66	128.38	128.70	128.89	15.850	15.890	15.913
28.31	128.25	128.58	128.76	13.807	13.842	13.861
31.85	128.17	128.49	128.681	12.272	12.303	12.321
35.53	128.11	128.43	128.618	11.001	11.029	11.044

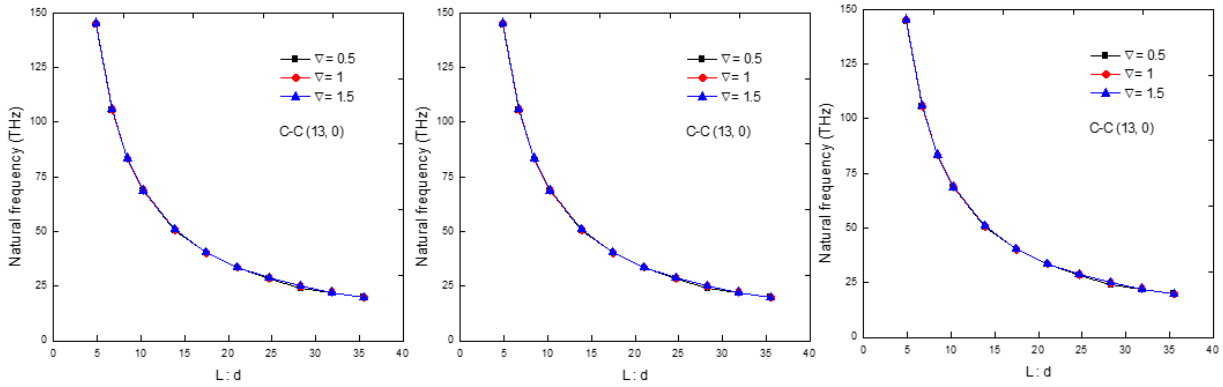

Fig. 3 Effect of C-C, SS-SS and C-F zigzag (13, 0), frequencies versus length-to-diameter ratio

SWCNTs, it can be seen that the effect of BCs is significant and more less prominent at shorter *L:d* = 5~15). It can take into account that the armchair SWCNTs (11, 11) with C-C condition have the prominent and highest frequencies and other BCs followed as SS-SS and C-F as shown in Fig. 4. It is also concluded that the frequency curves with changing the values of *L:d* of C-F boundary condition are the lowest outcomes. It can also be reported from Figs. 3 and 4, that the outcomes of frequency response of armchair with prescribed boundary conditions are higher than that of zigzag frequency values. The variations of power law index ∇ for frequencies (Hz) of carbon nanotubes for BCs have

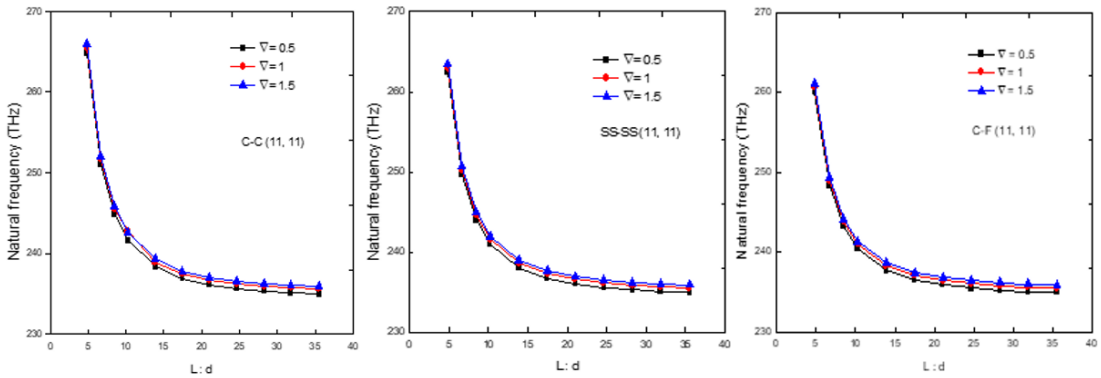

Fig. 4 Effect of C-C, SS-SS and CF (11, 11), frequencies versus length-to-diameter ratio

been sketched in graphs. As evidenced by these figures, the fundamental natural frequencies would slightly increase by increasing power law index ∇ for different BCs. For initial values, the gap between frequency curves is little significant and for bigger values of ratio *L:d*, the frequency curves moderately pronounced.

4. Conclusions

The fundamental natural frequency of SWCNTs versus ratio of length-to-diameter for a wide range has been reported and investigated through the study with specified boundary conditions. The modified Love shell theory with polynomial law for the CNTs vibrations provides a governing equation. Throughout the computations, on decreasing the length-to-diameter ratios, the frequencies of said structure increases. Effects of polynomial law for different ratios of length-to diameter versus fundamental natural frequencies been determined for two categories SWCNTs. Throughout the computation, frequency behavior for the boundary condition follow as; C-C, SS-SS frequency curves are higher than that of C-F curves. It is noted that with higher aspect ratio, the boundary conditions have a momentous influence on vibration of CNT. It can be concluded that frequencies would increase by increasing the power law index. This means that smaller effects play an important role in predicting SWCNT frequencies. For future concerns, the present Love's equations can be solved by using Ritz method.

Declaration of conflicting interests

The author(s) declared no potential conflicts of interest with respect to the research, authorship, and/or publication of this article.

Acknowledgments

The research team thanks the efforts of King Khalid University in financing this applied research and providing all the facilities (laboratories, hardware, and software) in the College of Engineering. In addition, special thanks to Civil Engineering Department where this applied research work achieved. Finally, thanks again to Deanship of Scientific Research in King Khalid University to continue to support scientific research until it becomes among the best universities locally and internationally. Within the framework of small research projects given by the Deanship of Scientific Research the grant number is 123.

References

Abdulrazzaq, M.A., Fenjan, R.M., Ahmed, R.A. and Faleh, N.M. (2020), "Thermal buckling of nonlocal clamped exponentially graded plate according to a secant function based refined theory", *Steel Compos. Struct., Int. J.*, **35**(1), 147-57. https://doi.org/10.12989/scs.2020.35.1.147.

Akbaş, Ş.D. (2015), "Wave propagation of a functionally graded beam in thermal environments", *Steel Compos. Struct., Int. J.*, **19**(6), 1421-1447. https://doi.org/10.12989/scs.2015.19.6.1421.

Akbaş, Ş.D. (2016a), "Forced vibration analysis of viscoelastic nanobeams embedded in an elastic medium", *Smart Struct. Syst., Int. J.*, **18**(6), 1125-1143. https://doi.org/10.12989/sss.2016.18.6.1125.

Akbaş, Ş.D. (2016b), "Analytical solutions for static bending of edge cracked micro beams", *Struct. Eng. Mech., Int. J.*, **59**(3), 579-599. http://dx.doi.org/10.12989/sem.2016.59.3.579.

Akbaş, Ş.D. (2016c), "Static analysis of a nano plate by using generalized differential quadrature method", *Int. J. Eng. Appl. Sci.*, **8**(2), 30-39. https://doi.org/10.24107/ijeas.252143.

Akbaş, Ş.D. (2017a), "Free vibration of edge cracked functionally graded microscale beams based on the modified couple stress theory", *Int. J. Struct. Stabil. Dyn.*, **17**(3), 1750033. https://doi.org/10.1142/S021945541750033X.

Akbaş, Ş.D. (2017b), "Forced vibration analysis of functionally graded nanobeams", *Int. J. Appl. Mech.*, **9**(7), 1750100. https://doi.org/10.1142/S1758825117501009.

Akbaş, S.D. (2018a), "Forced vibration analysis of cracked functionally graded microbeams", *Adv. Nano Res., Int. J.*, **6**(1), 39-55. http://dx.doi.org/10.12989/anr.2018.6.1.039.

Akbaş, Ş.D. (2018b), "Forced vibration analysis of cracked nanobeams", *J. Braz. Soc. Mech. Sci. Engineering*, **40**(8), 392. https://doi.org/10.1007/s40430-018-1315-1.

Akbaş, Ş.D. (2018c), "Bending of a cracked functionally graded nanobeam", *Adv. Nano Res., Int. J.*, **6**(3), 219-242. https://doi.org/10.12989/anr.2018.6.3.219.

Akbaş, Ş.D. (2019a), "Longitudinal forced vibration analysis of porous a nanorod", *Mühendislik Bilimleri Tasarım Dergisi*, **7**(4),

736-743. https://doi.org/10.21923/jesd.553328.

Akbaş, Ş.D. (2019b), "Axially forced vibration analysis of cracked a nanorod", *J. Comput. Appl. Mech.*, **50**(1), 63-68. https://doi.org/10.22059/jcamech.2019.281285.392.

Akbaş, Ş.D. (2020), "Modal analysis of viscoelastic nanorods under an axially harmonic load", *Adv. Nano Res., Int. J.*, **8**(4), 277-282. http://dx.doi.org/10.12989/anr.2020.8.4.277.

AlSaleh, R.J. and Fuggini, C. (2020), "Combining GPS and accelerometers' records to capture torsional response of cylindrical tower", *Smart Struct. Syst., Int. J.*, **25**(1), 111-122. https://doi.org/10.12989/sss.2020.25.1.111.

Arani, A.G., Kolahchi, R. and Esmailpour, M. (2016), "Nonlinear vibration analysis of piezoelectric plates reinforced with carbon nanotubes using DQM", *Smart Struct. Syst., Int. J.*, **18**(4), 787-800. http://dx.doi.org/10.12989/sss.2016.18.4.787.

Arefi, M. and Zenkour, A.M. (2017), "Nonlinear and linear thermo-elastic analyses of a functionally graded spherical shell using the Lagrange strain tensor", *Smart Struct. Syst., Int. J.*, **19**(1), 33-38. https://doi.org/10.12989/sss.2017.19.1.033.

Avcar, M. (2019), "Free vibration of imperfect sigmoid and power law functionally graded beams", *Steel Compos. Struct., Int. J.*, **30**(6), 603-615. https://doi.org/10.12989/scs.2019.30.6.603.

Batou, B., Nebab, M., Bennai, R., Atmane, H.A., Tounsi, A. and Bouremana, M. (2019), "Wave dispersion properties in imperfect sigmoid plates using various HSDTs", *Steel Compos. Struct., Int. J.*, **33**(5), 699-716. https://doi.org/10.12989/scs.2019.33.5.699.

Benmansour, D.L., Kaci, A., Bousahla, A.A., Heireche, H., Tounsi, A., Alwabli, A.S., Alhebshi, A.M., Al-ghmadi, K. and Mahmoud, S.R. (2019), "The nano scale bending and dynamic properties of isolated protein microtubules based on modified strain gradient theory", *Adv. Nano Res., Int. J.*, **7**(6), 443-457. https://doi.org/10.12989/anr.2019.7.6.443.

Bensattalah, T., Bouakkaz, K., Zidour, M. and Daouadji, T.H. (2018), "Critical buckling loads of carbon nanotube embedded in Kerr's medium", *Adv. Nano Res., Int. J.*, **6**(4), 339-356. https://doi.org/10.12989/anr.2018.6.4.339

Duan, W.H., Wang, C.M. and Zhang, Y.Y. (2007), "Calibration of nonlocal scaling effect parameter for free vibration of carbon nanotubes by molecular dynamic", *J. Appl. Phys.*, **101**(2), 024305. https://doi.org/10.1063/1.2423140.

Ebrahimi, F., Dabbagh, A., Rabczuk, T. and Tornabene, F. (2019), "Analysis of propagation characteristics of elastic waves in heterogeneous nanobeams employing a new two-step porosity-dependent homogenization scheme", *Adv. Nano Res., Int. J.*, **7**(2), 135-143. https://doi.org/10.12989/anr.2019.7.2.135.

Eltaher, M.A., Almalki, T.A., Ahmed, K.I. and Almitani, K.H. (2019), "Characterization and behaviors of single walled carbon nanotube by equivalent-continuum mechanics approach", *Adv. Nano Res., Int. J.*, **7**(1), 39-49. https://doi.org/10.12989/anr.2019.7.1.039.

Fenjan, R.M., Moustafa, N.M. and Faleh, N.M. (2020), "Scale-dependent thermal vibration analysis of FG beams having porosities based on DQM", *Adv. Nano Res., Int. J.*, **8**(4), 283-292. https://doi.org/10.12989/anr.2020.8.4.283.

Flugge, S. (1973), *Stresses in Shells*, Springer, Berlin, Germany.

Flügge, W. (1962), *Stresses in Shells Second Edition*, Springer-Verlag, Berlin, Germany.

Forsberg, K. (1962), "Influence of boundary conditions on modal characteristics of cylindrical shells", *J. Am. Inst. Aero. Astro.*, **2**, 182-189.

Gao, Y. and An, L. (2010), "A nonlocal elastic anisotropic shell model for microtubule buckling behaviors in cytoplasm", *Physica E Low Dimens. Syst. Nanostruct.*, **42**(9), 2406-2415. https://doi.org/10.1016/j.bbrc.2009.07.042.

Gibson, R.F., Ayorinde, E.O. and Wen, Y.F. (2007), "Vibrations of carbon nanotubes and their composites: A review", *Compos. Sci. Technol.*, **67**(1), 1-28. https://doi.org/10.1016/j.compscitech.2006.03.031.

Hamidi, A., Zidour, M., Bouakkaz, K. and Bensattalah, T. (2018), "Thermal and small-scale effects on vibration of embedded armchair single-walled carbon nanotubes", *J. Nano Res.*, **51**, 24-38. https://doi.org/10.4028/www.scientific.net/JNanoR.51.24.

Han, J., Globus, A., Jaffe, R. and Deardorff, G. (1997), "Molecular dynamics simulations of carbon nanotube-based gears", *Nanotechnology*, **8**(3), 95. https://doi.org/10.1088/0957-4484/8/3/001.

Heydarpour, Y., Aghdam, M.M. and Malekzadeh, P. (2014), "Free vibration analysis of rotating functionally graded carbon nanotube-reinforced composite truncated conical shells", *Compos. Struct.*, **117**, 187-200. http://doi.org/10.1016/j.compstruct.2014.06.023.

Jorio, A., Saito, R., Hafner, J.H., Lieber, C.M., Hunter, M., McClure, T., Dresselhaus, G., Dresselhaus, M.S. (2001), "Structural (n, m) determination of isolated single-wall carbon nanotubes by resonant Raman scattering", *Phys. Rev. Lett.*, **86**(6), 1118-1121. https://doi.org/10.1103/PhysRevLett.86.1118.

Kotakoski, J., Krasheninnikov, A.V. and Nordlund, K. (2006), "Energetics, structure and long-range interaction of vacancytype defects in carbon nanotubes: Atomistic simulations", *Phys. Rev. B*, **74**, 245420. https://doi.org/10.1103/PhysRevB.74.245420.

Krommer, M., Vetyukova, Y. and Staudigl, E. (2016), "Nonlinear modelling and analysis of thin piezoelectric plates: buckling and post-buckling behavior", *Smart Struct. Syst., Int. J.*, **18**(1), 155-181. https://doi.org/10.12989/sss.2016.18.1.155.

Kulathunga, D.D.T.K., Ang, K.K. and Reddy, J.N. (2009), "Accurate modeling of buckling of single-and double-walled carbon nanotubes based on shell theories", *J. Phys. Condens. Matter*, **21**(43), 435301. https://doi.org/10.1088/0953-8984/21/43/435301.

Lee, S.Y., Huynh, T.C., Dang, N.L. and Kim, J.T. (2019), "Vibration characteristics of caisson breakwater for various waves, sea levels, and foundations", *Smart Struct. Syst., Int. J.*, **24**(4), 525-539. https://doi.org/10.12989/sss.2019.24.4.525.

Madani, H. Hosseini, H. and Shokravi, M. (2016), "Differential cubature method for vibration analysis of embedded FG-CNT-reinforced piezoelectric cylindrical shells subjected to uniform and non-uniform temperature distributions", *Steel Compos. Struct., Int. J.*, **22**(4), 889-913. https://doi.org/10.12989/scs.2016.22.4.889.

Moazzez, K., Googarchin, H.S. and Sharifi, S.M.H. (2018), "Natural frequency analysis of a cylindrical shell containing a variably oriented surface crack utilizing line-spring model", *Thin-Wall. Struct.*, **125**, 63-75. https://doi.org/10.1016/j.tws.2018.01.009.

Moghadam, R.M., Hosseini, S.A. and Salehi, M. (2014), "The influence of stone-thrower-wales defect on vibrational characteristics of single-walled carbon nanotubes incorporating Timoshenko beam element", *Physica E Low Dimens. Syst. Nanostruct.*, **62**, 80-89. https://doi.org/10.1016/j.physe.2014.04.008.

Natsuki, T., Endo, M. and Tsuda, H. (2006), "Vibration analysis of embedded carbon nanotubes using wave propagation approach", *J. Appl. Phys.*, **99**(3), 034311. https://doi.org/10.1063/1.2170418.

Nebab, M., Atmane, H.A., Bennai, R. and Tahar, B. (2019), "Effect of nonlinear elastic foundations on dynamic behavior of FG plates using four-unknown plate theory", *Earthq. Struct., Int. J.*, **17**(5), 447-462. https://doi.org/10.12989/eas.2019.17.5.447.

Paliwal, D.N., Kanagasabapathy, H. and Gupta, K.M. (1995), "The large deflection of an orthotropic cylindrical shell on a Pasternak foundation", *Compos. Struct.*, **31**(1), 31-37. https://doi.org/10.1016/0263-8223(94)00068-9.

Poplawski, B., Mikulowski, G., Pisarski, D., Wiszowaty, R. and Jankowski, L. (2019), "Optimum actuator placement for damping of vibrations using the prestress-accumulation release control approach", *Smart Struct. Syst., Int. J.*, **24**(1), 27-35. https://doi.org/10.12989/sss.2019.24.1.027.

Rouhi, H., Ansari, R. and Arash, B. (2013), "Vibration analysis of double-walled carbon nanotubes based on the non-local donnell shell via a new numerical approach", *Int J. Mech. Sci.*, **37**, 91-105.

Safaei, B., Khoda, F.H. and Fattahi, A.M. (2019), "Non-classical plate model for single-layered graphene sheet for axial buckling", *Adv. Nano Res., Int. J.*, **7**(4), 265-275. https://doi.org/10.12989/anr.2019.7.4.265.

Salah, F., Boucham, B., Bourada, F., Benzair, A., Bousahla, A.A. and Tounsi, A. (2019), "Investigation of thermal buckling properties of ceramic-metal FGM sandwich plates using 2D integral plate model", *Steel Compos. Struct., Int. J.*, **33**(6), 805-822. https://doi.org/10.12989/scs.2019.33.6.805.

Selim, M.M. (2010), "Torsional vibration of carbon nanotubes under initial compression stress", *Braz. J. Phys.*, **40**(3), 283-287. http://dx.doi.org/10.1590/S0103-97332010000300004.

Semmah, A., Heireche, H., Bousahla, A.A. and Tounsi, A. (2019), "Thermal buckling analysis of SWBNNT on Winkler foundation by non local FSDT", *Adv. Nano Res., Int. J.*, **7**(2), 89-98. http://dx.doi.org/10.12989/anr.2019.7.2.089.

Shahsavari, D., Karami, B. and Janghorban, M. (2019), "Size-dependent vibration analysis of laminated composite plates", *Adv. Nano Res., Int. J.*, 7(5), 337-349. https://doi.org/10.12989/anr.2019.7.5.337.

Shen, H.S. (2009), "Nonlinear bending of functionally graded carbon nanotube-reinforced composite plates in thermal environments", *Compos. Struct.*, **91**, 9-19. https://doi.org/10.1016/j.compstruct.2009.04.026.

Sodel, W. (1981), *Vibration of Shell and Plates*, Mechanical Engineering Series, New York, USA.

Tohidi, H., Hosseini-Hashemi, S.H. and Maghsoudpour, A. (2018), "Size-dependent forced vibration response of embedded micro cylindrical shells reinforced with agglomerated CNTs using strain gradient theory", *Smart Struct. Syst., Int. J.*, **22**(5), 527-546. https://doi.org/10.12989/sss.2018.22.5.527.

Usuki, T. and Yogo, K. (2009), "Beam equations for multi-walled carbon nanotubes derived from Flugge shell theory", *Proc. Royal Soc. A.*, **465**(2104), 1199-1226. https://doi.org/10.1098/rspa.2008.0394.

Wang, J. and Gao, Y. (2016), "Nonlocal orthotropic shell model applied on wave propagation in microtubules", *Appl. Math. Model.*, **40**(11-12), 5731-5744. https://doi.org/10.1016/j.apm.2016.01.013.

Wang, V. and Liew, K.M. (2007), "Application of nonlocal continuum mechanics to static analysis of micro-and nanostructures", *Phys. Lett. A*, **363**, 236-242. http://dx.doi.org/10.1016/j.physleta.2006.10.093.

Warburton, G.B. (1965), "Vibration of thin cylindrical shells", *J. Mech. Eng. Sci.*, **7**(4), 399-407. https://doi.org/10.1243/JMES_JOUR_1965_007_062_02.

Xuebin, L. (2008), "Study on free vibration analysis of circular cylindrical shells using wave propagation", *J. Sound Vib.*, **311**, 667-682. https://doi.org/10.1016/j.jsv.2007.09.023.

Yeh, J.Y. (2016), "Vibration characteristic analysis of sandwich cylindrical shells with MR elastomer", *Smart Struct. Syst., Int. J.*, **18**(2), 233-247. https://doi.org/10.12989/sss.2016.18.2.233.

Zahrai, S.M. and Kakouei, S. (2019), "Shaking table tests on a SDOF structure with cylindrical and rectangular TLDs having rotatable baffles", *Smart Struct. Syst., Int. J.*, **24**(3), 391-401. https://doi.org/10.12989/sss.2019.24.3.391.

Zhang, Y.Y., Wang, C.M. and Tan, V.B.C. (2009), "Assessment of Timoshenko beam models for vibrational behavior of singlewalled carbon nanotubes using molecular dynamics", *Adv. Appl. Math. Mech.*, **1**, 89-106.

Zou, R.D. and Foster, C.G. (1995), "Simple solution for buckling of orthotropic circular cylindrical shells", *Thin-Wall. Struct.*, **22**(3), 143-158. https://doi.org/10.1016/0263-8231(94)00026-V.

CC

Appendix-I

$$\sigma_{11} = F_{11}\frac{\partial^2}{\partial x^2} + \left(\frac{F_{66}}{R^2} + \varepsilon_t\right)\frac{\partial^2}{\partial \theta^2}$$

$$\sigma_{12} = \frac{(F_{12}+F_{66})}{R}\frac{\partial^2}{\partial x \partial \theta} + \frac{(G_{12}+2G_{66})}{R^2}\frac{\partial^2}{\partial x \partial \theta}$$

$$\sigma_{13} = \left(\frac{F_{12}}{R} - \varepsilon_t R\right)\frac{\partial}{\partial x} - G_{11}\frac{\partial^3}{\partial x^3} - \frac{(G_{12}+2G_{66})}{R^2}\frac{\partial^3}{\partial x \partial \theta^2}$$

$$\sigma_{21} = \left(\frac{F_{12}+F_{66}}{R} + \frac{G_{12}+G_{66}}{R^2} + \varepsilon_t R\right)\frac{\partial^2}{\partial x \partial \theta}$$

$$\sigma_{22} = \left(F_{66} + \frac{3G_{66}}{R} + \frac{2K_{66}}{R^2}\right)\frac{\partial^2}{\partial x^2} + \left(\frac{F_{22}}{R^2} + \frac{2G_{22}}{R^3} + \frac{K_{22}}{R^4}\right)\frac{\partial^2}{\partial \theta^2} + \varepsilon_t$$

$$\sigma_{23} = \left(\frac{F_{22}}{R^2} + \frac{G_{22}}{R^3}\right)\frac{\partial}{\partial \theta} - \left(\frac{G_{22}}{R^3} + \frac{K_{22}}{R^4}\right)\frac{\partial^3}{\partial \theta^3} - \left(\frac{G_{12}+2G_{66}}{R} + \frac{K_{12}+2K_{66}}{R^2}\right)\frac{\partial^3}{\partial x^2 \partial \theta} - 2\varepsilon_t\frac{\partial}{\partial t}$$

$$\sigma_{31} = -\frac{F_{12}}{R}\frac{\partial}{\partial x} + G_{11}\frac{\partial^3}{\partial x^3} + \left(\frac{G_{12}+2G_{66}}{R^2}\right)\frac{\partial^3}{\partial x \partial \theta^2}$$

$$\sigma_{32} = -\left(\frac{F_{22}}{R^2} + \frac{G_{22}}{R^3} + \varepsilon_t\right)\frac{\partial}{\partial \theta} + \left(\frac{G_{22}}{R^3} + \frac{K_{22}}{R^4}\right)\frac{\partial^3}{\partial \theta^3} + \left(\frac{G_{12}+2G_{66}}{R} + \frac{K_{12}+4K_{66}}{R^2}\right)\frac{\partial^3}{\partial x^2 \partial \theta} + 2\varepsilon_t\frac{\partial}{\partial t}$$

$$\sigma_{33} = -\frac{F_{22}}{R^2} + \varepsilon_t + \frac{2G_{12}}{R}\frac{\partial^2}{\partial x^2} + \left(\frac{2G_{22}}{R^3} + \varepsilon_t\right)\frac{\partial^2}{\partial \theta^2} - G_{11}\frac{\partial^4}{\partial x^4} - 2\left(\frac{K_{12}+2K_{66}}{R^2}\right)\frac{\partial^4}{\partial x^2 \partial \theta^2} - \frac{K_{22}}{R^4}\frac{\partial^4}{\partial \theta^4}$$

where

$$I_1 = \int_0^L \frac{d^3\chi}{dx^3}\frac{d\chi}{dx}dx, \qquad I_2 = \int_0^L \frac{d\chi}{dx}\frac{d\chi}{dx}dx$$

$$I_3 = \int_0^L \frac{d^2\chi}{dx^2}\chi(x)dx, \qquad I_4 = \int_0^L \chi(x)\chi(x)dx$$

$$I_5 = \int_0^L \frac{d^4\chi}{dx^4}\chi(x)dx, \qquad I_6 = \int_0^L \frac{d\chi}{dx}\frac{d\chi}{dx}dx$$

$$I_7 = \int_0^L \chi(x)\frac{d\chi}{dx}dx, \qquad I_8 = \int_0^L \frac{d^3\chi}{dx^3}\frac{d\chi}{dx}dx$$

$$I_9 = \int_0^L \frac{d^2\chi}{dx^2}\frac{d\chi}{dx}dx, \qquad I_{10} = \int_0^L \chi(x)\chi(x)\,dx$$

$$I_{11} = \int_0^L \frac{d^2\chi}{dx^2}\chi(x)dx, \qquad I_{12} = I_7$$

$$I_{13} = \int_0^L \chi^2(x)\,dx, \qquad I_{14} = \int_0^L \frac{d^2\chi}{dx^2}\chi(x)\,(x-a)^2dx$$

$$I_{15} = \int_0^L \frac{d\chi}{dx}\chi(x)dx, \qquad I_{16} = \int_0^L \frac{d^4\chi}{dx^4}\chi(x)dx$$

$$I_{17} = \int_0^L \frac{d^3\chi}{dx^3}\chi(x)dx, \qquad I_{18} = \int_0^L \frac{d^2\chi}{dx^2}\chi(x)dx$$

$$I_{19} = \int_0^L \frac{d^4\chi}{dx^4}\chi(x)dx$$